

# ELECTRO-MAGNETIC OPTIMIZATION OF A HALF-WAVE RESONATOR\*

B. Mustapha<sup>#</sup>, A. A. Kolomiets, Z. A. Conway, and P. N. Ostroumov, ANL, Argonne, IL 60439, USA

## Abstract

The optimization procedure developed for the electromagnetic (EM) design of a quarter-wave resonator (QWR) optimized for  $\beta = 0.077$  for an ATLAS upgrade has now been successfully tested. This prototype QWR achieved record peak surface fields for low-beta cavities of 70 MV/m and 105 mT and is capable of providing a voltage gain of 4.4 MV, far exceeding the design voltage of 2.5 MV. We have developed and applied a similar procedure for the EM design of a 322 MHz,  $\beta \sim 0.29$  half-wave resonator (HWR) for the medium energy section of the FRIB driver linac. The optimization approach and the final results will be described. The choice of aperture and its effect on the EM design parameters will be discussed. A comparison between equivalent half-wave and single-spoke resonators will also be presented. The transition from the electromagnetic model in Microwave Studio to the engineering model in the CAD program Inventor was carefully studied as it may affect both the EM design parameters and the cavity fabrication.

## INTRODUCTION

The FRIB driver linac design [1] is based on quarter-wave resonators (QWR) in the low-energy section and half-wave resonators (HWR) in the medium and high-energy sections. The recent SRF developments at Argonne [2] showed that the design and production of these structures could be very well optimized to achieve record high accelerating voltage. A procedure, similar to the one used for the design optimization of the QWR for the ATLAS intensity upgrade [3], was developed for the electromagnetic design optimization of a 322 MHz HWR for the medium-energy section of the FRIB driver linac. In this section, a uranium beam is accelerated from 16 to 55 MeV/u, with a  $\beta_{\text{opt}} \sim 0.29$  for the HWR. The mechanical and engineering design is reported in a separate contribution [4].

## HWR GEOMETRY: CHOICES, CONSTRAINTS AND PARAMETERS

Following the success of the conical QWR developed for the ATLAS upgrade [3], we chose a (double) conical shape for this HWR. A conical HWR has been proposed and studied before [5,6] but never built. Both the outer and inner conductors are conical giving the cavity the “hour-glass” shape shown in figure 1. The cavity outer shell (CV) middle section is cylindrical while the inner conductor (IC) has a race-track central section. The inner conductor and outer shell are joined with two toroidal

sections on the top and bottom. The drift tube (DT) re-entrant nose is also of conical shape. These choices are based on preliminary shape optimization. Figure 1 shows the most important geometry parameters used in the optimization and Table 1 gives their description. It is worth noting that other dimensions like the drift tube penetration depth (DTPN) and the inner conductor race-track width (ICRTZ) are fully determined from the cavity middle radius (CVMR), the mid-gap distance (MGD) and the gap width (GapW) and they are not directly used in the optimization.

In addition to the choices made above, we have to consider a several constraints. Some of these constraints are purely geometric; others are based on the manufacturing experience of the ATLAS intensity upgrade QWR. The main constraints are:

- 1) The inner conductor top radius (ICTR) was varied to study its effect then set to the QWR value of 8 cm due to manufacturing considerations.
- 2) The inner and outer conductor cones are required to end with short flat cylindrical sections for frequency adjustment cuts.
- 3) The distance between gap centres (MGD) is fixed to approximately half the wave length at the design  $\beta_G$ ,  $MGD \sim \beta_G \lambda / 2$  to have  $\beta_{\text{opt}} \sim 0.29$ .
- 4) The difference between the cavity top (CVTR) and middle (CVMR) radii should not exceed 5 cm to take advantage of cavities interconnections without additional real-estate to fit the larger top.

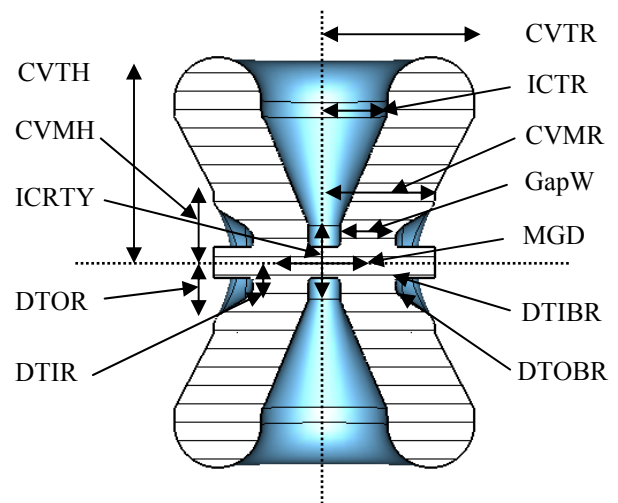


Figure 1: HWR cavity geometry and parameters used in the electro-magnetic optimization.

This work was supported by the U.S. Department of Energy, Office of Nuclear Physics, under Contract No. DE-AC02-06CH11357 and WFO85Y64 Supported by Michigan State University.

<sup>#</sup>brahim@anl.gov

Table 1: Important geometry parameters: names and descriptions.

Parameter	Name
Mid-Gap Distance	MGD
Gap Width	GapW
Cavity Aperture Radius	CVAPR
Cavity Half Height	CVTH
Cavity Middle Section Half Height	CVMH
Cavity Middle Section Radius	CVMR
Cavity Top Radius	CVTR
IC Top Radius	ICTR
IC Race Track Half Length	ICRTX
IC Race Track Half Height	ICRTY
DT Reentrant Nose Outer Radius	DTOR
DT Reentrant Nose Inner Radius	DTIR
DT Outer Blending Radius	DTOBR
DT Inner Blending Radius	DTIBR

## ELECTRO-MAGNETIC DESIGN OPTIMIZATION

The goal of the optimization is to reach an accelerating voltage of 2.5 MV per cavity or higher at 75 mT and 42 MV/m peak fields. The optimization should minimize the peak surface fields ( $E_{peak}$  and  $B_{peak}$ ) and maximize the Shunt impedance ( $R/Q$ ) and the geometry factor ( $G=R_s \cdot Q$ ) of the cavity. The software used in these simulations is Microwave Studio from CST [7]. For fast turn-around, all the simulations were performed using  $2 \cdot 10^5$  mesh cells. Although the peak surface fields may not be accurate with this mesh, the relative change of their values with the geometry parameters is stable enough to guide the optimization procedure. For verification, the final geometries are simulated with  $2 \cdot 10^6$  mesh cells or more.

Studying the dependence of the RF parameters on the geometry parameters of table 1, we obtained the results in figure 2 showing the relative RF parameters change in % as a function of each geometry parameter. The results show that the peak electric field  $E_{peak}$  is more sensitive to the parameters of the middle section: CVMR, ICRTX, ICRTY, DTOBR, DTIR, DTIBR and GapW. The peak magnetic field  $B_{peak}$  and the  $R/Q$  ratio are more sensitive to the geometry parameters affecting the cavity volume: CVMR, CVMH, CVTR, ICTR, ICRTX and ICRTY. The geometry factor  $G$  is more sensitive to the major geometry parameters CVTR and ICTR. We should note in particular that making the cavity middle section larger by few centimetres (CVMR: 13  $\rightarrow$  15 cm) the peak surface fields drop by more than 10% and the  $R/Q$  ratio increases by more than 15%. Similarly increasing the cavity top

size (CVTR: 18  $\rightarrow$  20 cm), increases the cavity geometry factor by about 10%. It is important to note that the optimization procedure is not mathematical with well defined goal function but rather a manual optimization based on the RF parameters response to changes in the geometry. Mapping the whole parameter space to find the global minimum would be very time-consuming, instead, at every iteration we vary all geometry parameters, identify the dominant one, fix it at its optimum value for the next iteration and repeat the same thing until a stable optimum solution is found. Although the geometry parameters used for the optimization are varied independently, their effects on the RF parameters are correlated and some parameter dependence of figure 2 may change along the optimization path.

Table 2 gives the initial and final geometry parameters before and after optimization and table 3 shows the corresponding RF parameters. Figure 3 shows the final geometry and the corresponding electric and magnetic field distributions. Note that the starting shape and parameters were chosen to be near an optimized solution based on previous experience, but the optimization procedure still led to the improvements indicated in table 3.

Table 2: Geometry parameters at the start and end of the optimization procedure. The end values are the results of the optimization.

Parameter	Start value (cm)	End value (cm)
MGD	11	10.6
GapW	7	7
CVAPR	2	2
CVTH	26	25
CVMH	7	9
CVMR	13	15
CVTR	18	20
ICTR	9	8
ICRTX	4.5	5
ICRTY	4.75	3.3
DTOR	7	7
DTIR	4	5.5
DTOBR	2	3.5
DTIBR	0.5	0.75

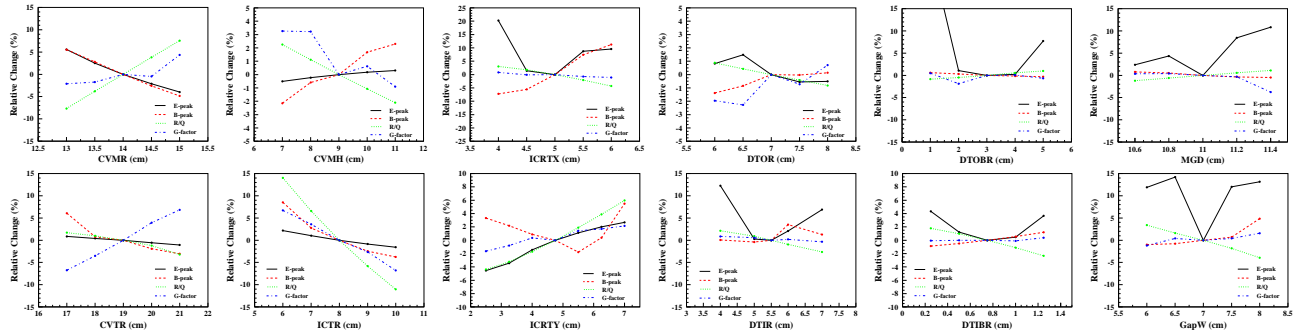


Figure 2: RF parameters dependence on the geometry parameters used for the optimization. The curves show relative RF parameters change in % as function of geometry parameters.

Table 3: RF parameters before and after optimization. The peak surface fields are normalized using the effective length  $L_{eff} = 27 \text{ cm} \sim \beta_{opt}\lambda$ .

RF Parameter	Start Value	End Value	Units
$E_{peak}/E_{acc}$	4.8	4.3	-
$B_{peak}/E_{acc}$	74	69	Gs/( MV/m)
R/Q	182	196	Ohm
$R_sQ$	83	95	Ohm

### COMPARISON TO THE EQUIVALENT SINGLE SPOKE RESONATOR

For the same velocity and frequency range, the single-spoke structure (SSR) is a competitive candidate. The main geometrical difference between a HWR and a SSR is that the former is a cylinder transverse to the beam axis while the later is a longitudinal cylinder; otherwise they both have a cross section similar to figure 1. We have reported earlier a general comparison between the HWR and SSR structures [8], but we emphasize here the geometric and electromagnetic aspects. For this comparison, the equivalent SSR was based on the optimized geometries of [9] with the geometry parameters listed in table 4 defined as for the HWR.

Table 4: Geometry parameters for the equivalent SSR.

Parameter	Name	Value
Mid-Gap Distance	MGD	10.6
Gap Width	GapW	7.0
Cavity Aperture	CVAPR	2
Cavity Outer Radius (Eq. CVTH)	CVOR	26
Cavity Half Length (Eq. CVTR)	CVLN	18
IC Top Radius	ICTR	9.8
IC Race Track Half Length	ICRTX	5.5
IC Race Track Half Height	ICRTY	3.3
DT Reentrant Nose Outer Radius	DTOR	12.9
DT Reentrant Nose Inner Radius	DTIR	5.5
DT Outer Blending Radius	DTOBR	3.5
DT Inner Blending Radius	DTIBR	0.75

The geometry and field distributions of the equivalent SSR are shown in figure 4. The corresponding RF parameters are compared to those of the HWR in table 5. We can see that the equivalent SSR has a significantly better R/Q ratio, making it capable to produce a given voltage with less power consumption. The rest of the parameters are comparable to the HWR values. The HWR was selected in this case for three main reasons:

- 1) Its conic shape, the HWR's foot-print on the beam line is shorter than the equivalent SSR increasing the real-estate gradient.
- 2) Ease of frequency tuning using geometry cuts included in the design.
- 3) Ease of processing by introducing special ports for electro-polishing after full assembly, which is not possible for SSR.

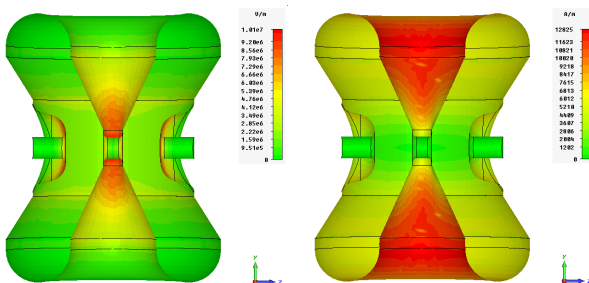


Figure 3: The final optimized geometry along with the electric (left) and magnetic (right) field distributions.

Table 5: Comparison of RF parameters for the HWR and the equivalent SSR.

RF Parameter	HWR	SSR	Units
$E_{\text{peak}}/E_{\text{acc}}$	4.3	4.0	-
$B_{\text{peak}}/E_{\text{acc}}$	69	61	Gs/( MV/m)
R/Q	196	229	Ohm
$R_sQ$	95	95	Ohm

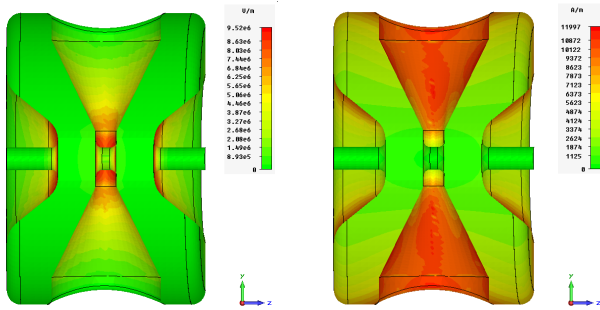


Figure 4: Geometry of the equivalent SSR along with the electric and magnetic field distributions.

If we use the actual cavity foot print along the beam axis instead of the effective length  $L_{\text{eff}} = \beta_{\text{opt}}\lambda$  to normalize the peak surface fields we obtain the results of table 6.

Table 6: Comparison of RF parameters for the HWR and the equivalent SSR with different normalization lengths.

RF Parameter	HWR	SSR	Units
$L_{\text{norm}}$	30	36	cm
$E_{\text{peak}}/E_{\text{acc}}$	4.8	5.4	-
$B_{\text{peak}}/E_{\text{acc}}$	77.3	81.4	Gs/( MV/m)
R/Q	196	229	Ohm
$R_sQ$	95	95	Ohm

In this way we factor the first selection argument of the HWR into the RF parameters, which we believe is a more realistic comparison of the equivalent HWR and SSR cavities. In this normalization, the HWR is more competitive for peak surfaces fields.

### APERTURE AND PORT EFFECTS

#### Aperture Choice and Its Effect

To accommodate potential emittance growth of high-intensity light-ion beams and multiple charge-state heavy ion beams in the FRIB driver linac, the aperture radius for this cavity was set to 2 cm. With a careful linac design, especially the most critical low- $\beta$  section, good alignment and efficient correction system, the emittance growth could be controlled to use a 1.5 cm aperture.

By simply changing the aperture radius to 1.5 cm, without further optimization, we obtain the results given in table 7. With a smaller aperture radius, the shunt impedance is enhanced while other parameters remain comparable. With further optimization, it may be possible to improve other RF parameters too.

Table 7: Comparison of RF parameters of the HWR with different aperture radii.

RF Parameter	CVAPR=2	CVAPR=1.5	Units
$E_{\text{peak}}/E_{\text{acc}}$	4.3	4.2	-
$B_{\text{peak}}/E_{\text{acc}}$	69	68	Gs/( MV/m)
R/Q	196	207	Ohm
$R_sQ$	95	95	Ohm

#### Magnetic Field Enhancement with Ports

When producing an Inventor model of the cavity, ports were added to the geometry; see figure 5. A MWS simulation used to verify the cavity RF parameters showed a significant enhancement in the peak magnetic field which was reduced by increasing the ports' blending radius (BR) as shown on figure 6. The standard value of the ports' BR used in the manufacturing of the QWR is 0.25" (0.635 cm); while it is possible to increase it to 0.5" (1.27 cm) it will be harder to go any further [10]. Table 8 compares the peak magnetic field before adding the ports to the case with ports and blending radii of 0.25" and 0.5". Figure 7 shows the corresponding magnetic field distribution on the toroid. It is important to note that this effect was not observed for the QWR which is probably due to its larger volume and larger inner conductor surface on which the magnetic field is spread.

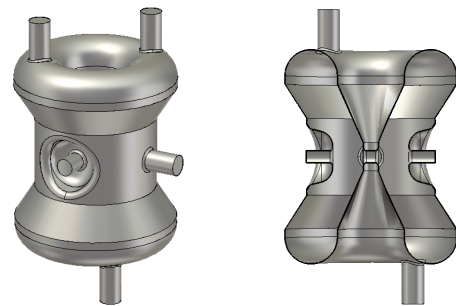


Figure 5: Inventor model with all ports.

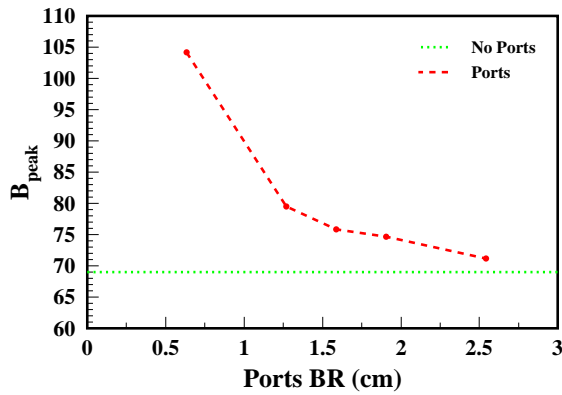


Figure 6: Peak magnetic field dependence on the ports blending radius. The horizontal line is the value before adding the ports.

Table 8: Comparison of peak magnetic field for the HWR with different blending radii around the ports.

Parameter	No Ports	BR=1/4" (0.635 cm)	BR=1/2" (1.27 cm)	Units
B <sub>peak</sub> /E <sub>acc</sub>	71	104	80	Gs/ (MV/m)

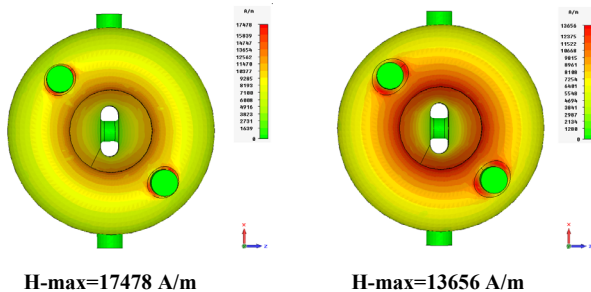


Figure 7: Magnetic field distribution on the cavity toroid after adding the ports with a blending radius of 0.25" (left) and 0.5" (right).

## SUMMARY

We have optimized the electromagnetic design of a 322 MHz -  $\beta \sim 0.29$  HWR for the medium-energy section of the FRIB driver linac. The cavity has an "hour-glass" shape with conical inner and outer conductors and is capable of delivering a 2.5 MV accelerating voltage with peak surface fields of 75 mT and 42 MV/m. A HWR was selected over a SSR for its shorter foot print on the beam line, ease of tuning during fabrication and ease of processing after full assembly. The design is now ready for prototyping.

## REFERENCES

- [1] R.C. York et al, "FRIB: A New Accelerator Facility for the Production of Rare Isotope Beams", Proceedings of SRF-09, Berlin, Germany, September 2009, p. 888.
- [2] M.P. Kelly and P.N. Ostroumov, "SRF Advances for ATLAS and other  $\beta < 1$  Applications", Invited paper THIOB04 in these proceedings.
- [3] B Mustapha and P.N. Ostroumov, "Electromagnetic Optimization of a Quarter-Wave Resonator", Proceedings of LINAC-10, Tsukuba, Japan, September 2010.
- [4] P.N. Ostroumov et al, " $\beta=0.285$  Half-Wave Resonator for FRIB", MOPO026, These proceedings.
- [5] J. Delayen "Design of Low Velocity SC Accelerating Structures Using Quarter Wavelength Resonant Lines", NIM A 259 (1987), 341-357.
- [6] E. Zaplatin, "Conical Half-Wave Resonator Investigations", Proceedings of SRF-09, Berlin, Germany, September 2009, p. 564.
- [7] CST: Computer Simulation Technology, www.cst.com
- [8] Z.A. Conway et al, "A Comparison of Superconducting RF Structures Optimized for  $\beta=0.285$ ", Proceedings of PAC-11, New York, USA, March 2011.
- [9] I. Gonin et al, "Single Spoke Cavities for Low-Energy Part of CW Linac of Project X", Proceedings of IPAC-10, Kyoto, Japan, May 2010.
- [10] J. Rathke (AES), private communication.